Histol Histopathol (2002) 17: 223-237

http://www.hh.um.es

Histology and Histopathology

Cellular and Molecular Biology

Identification of dendritic cells in aortic atherosclerotic lesions in rats with diet-induced hypercholesterolaemia

J. Ozmen[1,2], Y.V. Bobryshev[1], R.S.A. Lord[1] and K.W.S. Ashwell[2]

[1]Surgical Professorial Unit, St. Vincent's Hospital, University of New South Wales, Sydney, Australia and

[2]School of Anatomy, University of New South Wales, Sydney, Australia

Summary. We have previously identified dendritic cells (DCs) in the intima of human large arteries. These vascular DCs are common in atherosclerotic lesions but their immature forms are also present in normal arterial intima. Pathophysiological studies on vascular DCs are limited because they have only been studied in human specimens obtained at operation or post-mortem. The aim of the current study was to determine whether DCs participate in the development of atherosclerotic lesions in hypercholesterolemic rats. Male Wistar rats were divided into a control (n=13) and experimental cohort (n=48). The experimental animals were fed an atherogenic diet and 1% saline, while the controls were fed standard rat cubes and water. The aortas were obtained from both groups at 10, 20, and 30 weeks following commencement of the diet. An *en face* immunohistochemical technique, routine section immunohistochemistry, and transmission electron microscopy were used to detect the presence of DCs in the aortas. Examination of the aortas showed that $S100^+$ cells with dendritic cell morphology were present in the aortic intima of hypercholesterolemic rats. The $S100^+$ DCs displayed immunopositivity for OX-62 and MHC Class II antibodies. Within various types of atherosclerotic lesions, these cells were clustered throughout the intima but were especially prominent around arterial branch-points where they co-localized with various cell types, including T-cells and macrophages. Ultrastructural analysis confirmed the presence of cells with characteristics typical of DCs. These features included the presence of a well-developed tubulovesicular system, dendritic processes, and a lack of secondary lysosomes and phagosomes. This study establishes the presence of DCs in the aortic intima of rats with diet-induced atherosclerosis. The presence of DCs in this model of experimental atherogenesis could provide a new approach to investigating the function of DCs and may help clarify the immune-inflammatory mechanisms underlying atherosclerosis.

Offprint requests to: Dr. Yuri V. Bobryshev, Surgical Professorial Unit, Level 17 O'Brien Building, St. Vincent's Hospital, Victoria Street, Darlinghurst NSW 2010, Australia. Fax: +61 2 9360 4424. e-mail: ybobryshev@stvincents.com.au

Key words: Atherosclerosis, Hypercholesterolaemia, Rat, Dendritic cells

Introduction

We have previously demonstrated the existence of dendritic cells (DCs) in the intima of human large arteries (Bobryshev and Lord, 1995a,b, 1996; Bobryshev et al., 1996a; Bobryshev, 2000). These vascular DCs are found in atherosclerotic plaques and in normal intima to a lesser extent (Bobryshev and Lord, 1995a,b; Bobryshev, 2000). Vascular DCs have ultrastructural features unique to DCs such as Langerhans cells and interdigitating cells (King and Katz, 1990; Steinman, 1991; Kamperdijk et al., 1993; Sprecher and Becker, 1993; Banchereau and Steinman, 1998), which include a well-developed tubulovesicular system, dendritic cellular processes, and a lack of secondary lysosomes and phagolysosomes. Vascular DCs express S100 protein (Bobryshev and Lord, 1995a,b; Bobryshev et al., 1996a), CD1a (Bobryshev and Lord, 1995b; Bobryshev et al., 1996a), HLA-DR (Bobryshev et al., 1996a), ICAM-1 (Bobryshev et al., 1996a), VCAM-1 (Bobryshev et al., 1996b), with either S100 or CD1a as adequate markers for their immunohistochemical identification in humans. Vascular DCs co-localize with T-cells, B-cells, and macrophages within atherosclerotic plaques, suggesting that they are involved in immunological reactions in the artery wall (Bobryshev and Lord, 1998). Little is known about the function of vascular DCs, but as members of the family of DCs they are expected to act as specialized antigen-presenting cells (Bobryshev and Lord, 1998).

The dendritic cell system of antigen-presenting cells is the initiator and modulator of the immune response and includes a diverse population of cells with different properties, differentiation and activation states (King and

Katz, 1990; Steinman, 1991; Kamperdijk et al., 1993; Sprecher and Becker, 1993; Banchereau and Steinman, 1998). DCs were first described in 1868 as Langerhans cells in the skin and because of their "tree-like" appearance these cells were designated DCs (Steinman and Cohn, 1973; Hart and Fabre, 1981). A more recent definition of DCs includes the ability of the cell to migrate and activate a primary T-cell response (Hart, 1997). DCs have the capacity to activate T-cells, while no other blood cell displays similar motility or similar ability to capture antigen and select antigen-specific T-lymphocytes (Banchereau and Steinman, 1998). DCs have a stellate appearance in situ and when examined under the scanning electron microscope exhibit long and thin spiny or sheet-like cellular processes, which can exceed 10 µm in length (Banchereau and Steinman, 1998). Other features of DCs include a lack of phagocytic function and the capacity to alter their activation state. Another property of DCs, unique to interdigitating cells of lymph nodes, is the tubulovesicular system, a system of tubules, cisterns, and vesicles, which facilitates the transport of various substances between the extracellular space and the intracellular compartment (Bobryshev et al., 1997; Hart, 1997). The most important feature of DCs is their powerful capacity for the uptake of antigen and the presentation of antigen to T-cells (Knight et al., 1985; Macatonia et al., 1987; Inaba et al., 1990; King and Katz, 1990; Pure et al., 1990; Steinman, 1991; Kamperdijk et al., 1993; Sprecher and Becker, 1993; Banchereau and Steinman, 1998). DCs are closely associated with T-lymphocytes and hence regulate immune responses through these connections (King and Katz, 1990; Steinman, 1991; Kamperdijk et al., 1993; Sprecher and Becker, 1993).

DCs exist in two functional states, as either immature or mature DCs (King and Katz, 1990; Steinman, 1991; Kamperdijk et al., 1993; Sprecher and Becker, 1993; Banchereau and Steinman, 1998). Maturing DCs are derived from bone marrow precursors (King and Katz, 1990; Steinman, 1991; Kamperdijk et al., 1993; Sprecher and Becker, 1993; Banchereau and Steinman, 1998). A minor percentage of these precursor forms leave the bone marrow and circulate in the bloodstream (Steinman et al., 1974). These circulating cells then leave the blood and enter the tissues, where they become interstitial DCs, like Langerhans cells of the skin (Romani and Schuler, 1992). Within the tissues, interstitial DCs have long cell processes and function as sentries. Once immature DCs capture antigen they undergo complete maturation and mobilization, only then being able to activate T-cells (Banchereau and Steinman, 1998). Unlike their mature forms, immature DCs are poorly equipped to present antigen and are better suited for capturing antigen, which is a key event in activating the immune system (Banchereau and Steinman, 1998). Antigens that can initiate dendritic cell maturation include microbial and inflammatory products such as bacteria (Winzler et al., 1997), lipopolysaccharide (Sallusto and Lanzavecchia, 1995), and cytokines IL-1, GM-CSF, and TNFα (Buelens et al., 1997). Following capture and processing of antigen, DCs display large quantities of MHC-peptide complexes on their surfaces and subsequently migrate from the tissues to reside in T-cell zones in draining lymph nodes, the spleen and other lymphoid tissues where they activate T-lymphocytes (Hart, 1997). The mature dendritic cell activates T-cells, which then completes the immune response by liaising with B-cells for antibody formation, macrophages for the production of cytokines, and target-cells for lysis (Banchereau and Steinman, 1998).

The function of DCs was largely unknown until mixed leukocyte reaction models for graft rejection were developed (Banchereau and Steinman, 1998). Models, in which DCs respond to a mismatch between donor and recipient MHC, and studies of transplant rejection have demonstrated that only a few DCs are required to stimulate a strong cell-mediated immune response, with only one dendritic cell needed to activate 100 to 3000 T-cells (Banchereau and Steinman, 1998). These and other observations have led to the current opinion that DCs are specialized initiators of the immune response (Banchereau and Steinman, 1998). Although it has long been accepted that antigens and lymphocytes play a pivotal role in immune defences, all the recent evidence places new emphasis on the role of DCs in regulating the immune system (Banchereau and Steinman, 1998).

Functional studies of dendritic cell involvement in atherosclerotic plaque formation has been limited because vascular DCs have mainly been examined in human arterial specimens obtained at operation and post-mortem. In a preliminary study, we noted the expression of S100 protein in atherosclerotic lesions in rats (Ozmen et al., 1998). The nature of the cells expressing S100 protein was unclear (Ozmen et al., 1998). The observation, however, suggested that DCs might participate in atherosclerotic lesion formation in hypercholesterolemic rats. The present study was undertaken to verify this hypothesis.

Materials and methods

The study was approved by the Animal Care and Ethics Committee, University of New South Wales (Ace No. 97/126).

Animals

The experiments were performed on 61 male Wistar rats of 8 to 10 weeks of age (Animal Breeding and Holding Unit, UNSW, Australia). The rats were housed in standard animal cages (three rats per cage) in an animal house with free access to food and water. The experimental rats (48 animals) were fed an atherogenic diet and 1% saline according to Belliveau and Marsh (1961). Control rats (13 animals) were fed standard rat pellets and water.

Tissue preparation

The animals were anaesthetized by intraperitoneal injection of pentobarbitone sodium 60 mg/kg. They were sacrificed after having been kept for 10, 20, and 30 weeks on the atherogenic diet (Table 1).

Blood samples (5 ml) were obtained from 20 and 30 weeks animals by percutaneous cardiac puncture for the estimation of serum total cholesterol and triglyceride levels. Blood cholesterol and triglyceride data was analyzed using a t-test (two-sample assuming unequal variances) to determine statistical significance.

The aortas were flushed with phosphate buffered saline pH 7.4 (PBS) at 4 °C for 5 min and then either perfused with freshly prepared solutions of 4% paraformaldehyde in PBS at 4 °C for 10 min (for paraffin sections and *en face* immunostaining) or 2.5% glutaraldehyde in 0.1M cacodylate buffer pH 7.4 at 4 °C for 10 min (transmission electron microscopy) or collected unfixed (frozen sections).

Paraffin sections

The aortas were fixed and prepared by perfusing with 4% paraformaldehyde in PBS at 4 °C for 10 min. The aortas, extending from the aortic arch to the iliac bifurcation, were divided into arch, thoracic, and abdominal segments, and immersed in the paraformaldehyde solution overnight at 4 °C. The aortic segments were dehydrated in an ethanol series and cleared with histolene and then processed in paraffin wax.

En face specimens

The aortas were fixed and prepared by perfusing with 4% paraformaldehyde in PBS at 4 °C for 10 min. The aortas, extending from the aortic arch to the iliac bifurcation, were dissected and immersed in the paraformaldehyde solution for 3 h at 4 °C. Under a Zeiss OPMI 99-Tragram dissecting microscope (X4 - X40), the adventitial layer of the aortas was removed by fine microdissecting scissors and forceps. The aortas were then divided into arch, thoracic and abdominal segments and split open longitudinally according to the protocol described by Haraoka and co-workers (1995). The aortic arch and thoracic segments were opened along the ventral side, while the abdominal segment was opened along the dorsal side, as the major arterial branches are located ventrally. The aortic segments were then progressively rinsed for 30 min each with 10%, 15%, and 20% sucrose in PBS, pH 7.4.

Frozen sections

Unfixed aortic specimens were washed in cold saline and embedded in O.C.T. compound and frozen in liquid nitrogen. The blocks were stored at -40 °C until sectioning.

Immunohistochemistry

Immunoperoxidase staining procedure for paraffin sections

After paraffin embedding, sections 5 µm thick were cut using a Microm HM325, collected on silanized slides, air dried for 30 min (60 °C) and immunolabelled by using the avidin-biotin complex (ABC)

Table 1. Number of animals used in the experiments.

WEEKS ON DIET	NUMER OF EXPERIMENTAL RATS	NUMBER OF CONTROL RATS	TOTAL NUMBER OF ANIMALS
10	16	4	20
20	16	5	21
30	16	4	20

Table 2. Antibodies used in the study.

NAME	TYPE[a]	SPECIES[b]	CLONE	MANUFACTURER	DILUTION	SPECIFICITY
S100	P	Rabbit	-	DAKO	1/600	Langerhans cells, interdigitating dendritic cells, *vascular dendritic cells*, glial cells, ependyma, Schwann cells
S100α	M	Mouse	SH-A1	Sigma BioSciences	1/250	S100 α-subunit
S100ß	M	Mouse	SH-B1	Sigma Immunochemicals	1/250	S100 ß-subunit
Dendritic cells	M	Mouse	MRC OX-62	Serotec	Neat	Rat dendritic cells, some γδ T-cells
MHC class II	M	Mouse	F17-23-2	Serotec	Neat	Rat class II MHC (antigen presenting cells)
CD4	M	Mouse	W3/25	Cedarlane	1/200	Rat helper T-cells
CD8	M	Mouse	MRC OX-8	Cedarlane	1/200	Rat cytotoxic/suppressor T-cells
Macrophage subset	M	Mouse	HIS 36	Pharmingen	1/150	Rat tissue macrophages, thioglycolate-elicited peritoneal exudate cells
SMA	M	Mouse	ASM-1	Novocastra	1/50	Smooth muscle cells

[a]: M, monoclonal antibody; P, polyclonal antibody. [b]: Species in which antibody is raised.

immunoperoxidase method according to Hsu and co-workers (1981). DCs were identified with anti-S100 (DAKO), T suppressor cells/cytotoxic T-cells with anti-rat CD8 (Cedarlane), T helper cells with anti-rat CD4 (Cedarlane), macrophages identified using an antibody to a rat macrophage subset (Pharmingen) and smooth muscle cells with antibody to alpha smooth muscle actin (Novocastra NCL-SMA). The working concentrations of the antibodies used are outlined in Table 2. Deparaffinised sections were immersed in PBS, pH 7.4, containing 3% hydrogen peroxide for 5 min, in order to eliminate endogenous peroxidase activity. The sections were treated with 0.1% trypsin or proteinase-K (for S100, SMA) in PBS for 5-10 min, or boiled in citrate buffer pH 6.0 (for CD4, CD8, Rat Macrophage Subset) to retrieve antigenicity. The sections were washed with tris-phosphate buffered saline, pH 7.6 (TPBS, 10 min), incubated with 1% normal goat serum (DAKO) for 5 min, and then incubated with the appropriate primary antibody for 1 h. After washing with TPBS for 10 min, the sections were incubated with the appropriate biotin-labeled secondary antibody (goat anti-rabbit, VECTOR BA-1000 or horse anti-mouse, VECTOR BA-2000) (1:100, 20 min). The sections were washed in TPBS for 10 min and then treated with avidin-biotin complex (ABC Elite Kit, VECTOR PK-6100) for 30 min. Brown-staining was produced by 2 min treatment with 3,3'-diaminobenzidine (50 mg/100ml PBS, pH 7.4, containing 0.01% hydrogen peroxide). All the incubations were performed at room temperature. After washing in tap water for 2 min, sections were counterstained in hematoxylin for 1 min and then washed in tap water for 2 min. The sections were dehydrated, cleared and mounted in Mount-Quick (Draido Sangyo Co. Ltd.). Sections were examined with the aid of an Olympus microscope at x4 to x100 magnifications. Adjacent sections not used for immunohistochemical reactions were stained with hematoxylin and eosin for morphological analysis.

Immunohistochemistry for frozen sections

Sections, 5 µm thick, were cut using a Shandon AS620 Cryotome and tested as previously. Sections were collected on silanized slides and allowed to air dry for 1 h at 60 °C, then fixed in 100% acetone (10 min, room temperature). Sections not required for immunohistochemistry on the day were stored in pure acetone at -40 °C until needed. Washing of sections in TBS (pH 7.6) for 10 min was then performed. Endogenous peroxidase activity was blocked for 15 min by immersing sections in 0.3% hydrogen peroxide in TPBS (pH 7.6). The sections were then transferred to TPBS (pH 7.6) for 5 min and then loaded onto a Sequenza slide holder (Shandon). Incubation of sections with normal goat serum (DAKO) (1:10, 5 min) was performed followed by incubation with the appropriate primary antibody for 1 h. DCs were identified with antibodies to S100 (DAKO), OX-62 (Serotec), and MHC Class II (Serotec). T suppressor cells/cytotoxic T-cells were stained with anti-rat CD8 (Cedarlane), T helper cells with anti-rat CD4 (Cedarlane), macrophages identified using an antibody to a rat macrophage subset (Pharmingen) and smooth muscle cells with antibody to alpha smooth muscle actin (Novocastra NCL-SMA). After washing with TPBS for 10 min, the sections were incubated with the appropriate biotin-labeled secondary antibody (goat anti-rabbit, VECTOR BA-1000 or horse anti-mouse, VECTOR BA-2000) (1:100, 20 min). The sections were washed in TPBS for 10 min and then treated with avidin-biotin complex (ABC Elite Kit, VECTOR PK-6100) for 30 min. Brown-staining was produced by 2 min treatment with 3,3'-diaminobenzidine (50 mg/100ml PBS, pH 7.4, containing 0.01% hydrogen peroxide). All the incubations were performed at room temperature. Following DAB detection, sections were washed in tap water for 2 min, and then counterstained in Methylene Blue for 1 min. The sections were washed in tap water for 2 min and stained in hematoxylin for 1 min, followed by washing in tap water for 2 min. The sections were dehydrated, cleared and mounted in Mount-Quick (Draido Sangyo Co. Ltd.). Sections were examined with the aid of an Olympus microscope and photomicrographs were taken at x40 to x200 magnifications. Semiquantitative analysis of cell composition in atherosclerotic lesions was carried out as previously (Bobryshev and Lord, 1998). Adjacent sections not used for immunohistochemical reactions were stained for morphological analysis with toluidine blue.

En face immunostaining procedure

For *en face* immunostaining the aortic segments were immersed in PBS, pH 7.4, containing 3% hydrogen peroxide for 5 min, in order to eliminate endogenous peroxidase activity. The segments were then laid flat on a special glass slide with the endothelium facing up and prepared for the application of appropriate solutions. After washing with TPBS, pH 7.6 (5 min) and incubation with normal goat serum (DAKO) (1:100, 15 min) the segments were incubated with anti-S100 for 1 h (DAKO, 1:600). The segments were washed (TPBS, 20 min) and incubated with biotin-labeled secondary antibody for 15 min (LSAB Kit, DAKO). After washing (TPBS, 20 min), the segments were treated with peroxidase-conjugated streptavidin for 15 min (LSAB Kit, DAKO). The peroxidase reaction was developed under an Olympus microscope with 3-amino-9-ethylcarbazole substrate-chromogen system (AEC substrate kit, DAKO). All procedures were undertaken at room temperature. The segments were rinsed with distilled water, mounted endothelium uppermost in a glycerin gel (Glycergel, DAKO) and examined by light microscopy.

Positive and negative controls

Positive controls were performed on rat skin sections

for antibodies to OX-62 and MHC Class II. The sections showed pronounced immunoreactivity (Fig. 1A, B). Other positive controls for S100, CD8, CD4, and rat macrophage HIS 36 antibodies were performed in rat para-aortic lymph nodes. The sections showed pronounced immunoreactivity (Figs. 1C-F).

For negative controls on both frozen and paraffin aortic sections, the first antibody was omitted or the sections were treated with an immunoglobulin fraction of non-immune goat serum (VECTOR S-1000) as a substitute for the primary antibody. None of the negative control sections showed positive immune staining. Negative staining for S100 and OX-62 is shown in Figs. 1G,H.

For *en face* specimens, omission of the primary antibody or pre-treatment with an immunoglobulin fraction of non-immune rabbit serum (1:100, DAKO) was used as negative controls (Fig. 1I).

Electron microscopy

The aortas for electron microscopic analysis were fixed and prepared by perfusing with PBS (4 °C) for 5 min and then 2.5% glutaraldehyde (4 °C) in 0.1M cacodylate buffer (pH 7.4) for 10 min. The aortas were dissected and cut into 5 mm segments for immersion fixation in 2.5% glutaraldehyde in 0.1M cacodylate buffer (pH 7.4) for 2 h at 4 °C. The segments were then washed in 0.1M cacodylate buffer (pH 7.4) overnight and postfixed the following day in 1% osmium tetroxide for 2 h at 4 °C. Specimens were washed in cacodylate buffer (pH 7.4) for 30 min and then block-stained with 2% uranyl acetate for 1 h at room temperature. Dehydration was performed using a graded ethanol

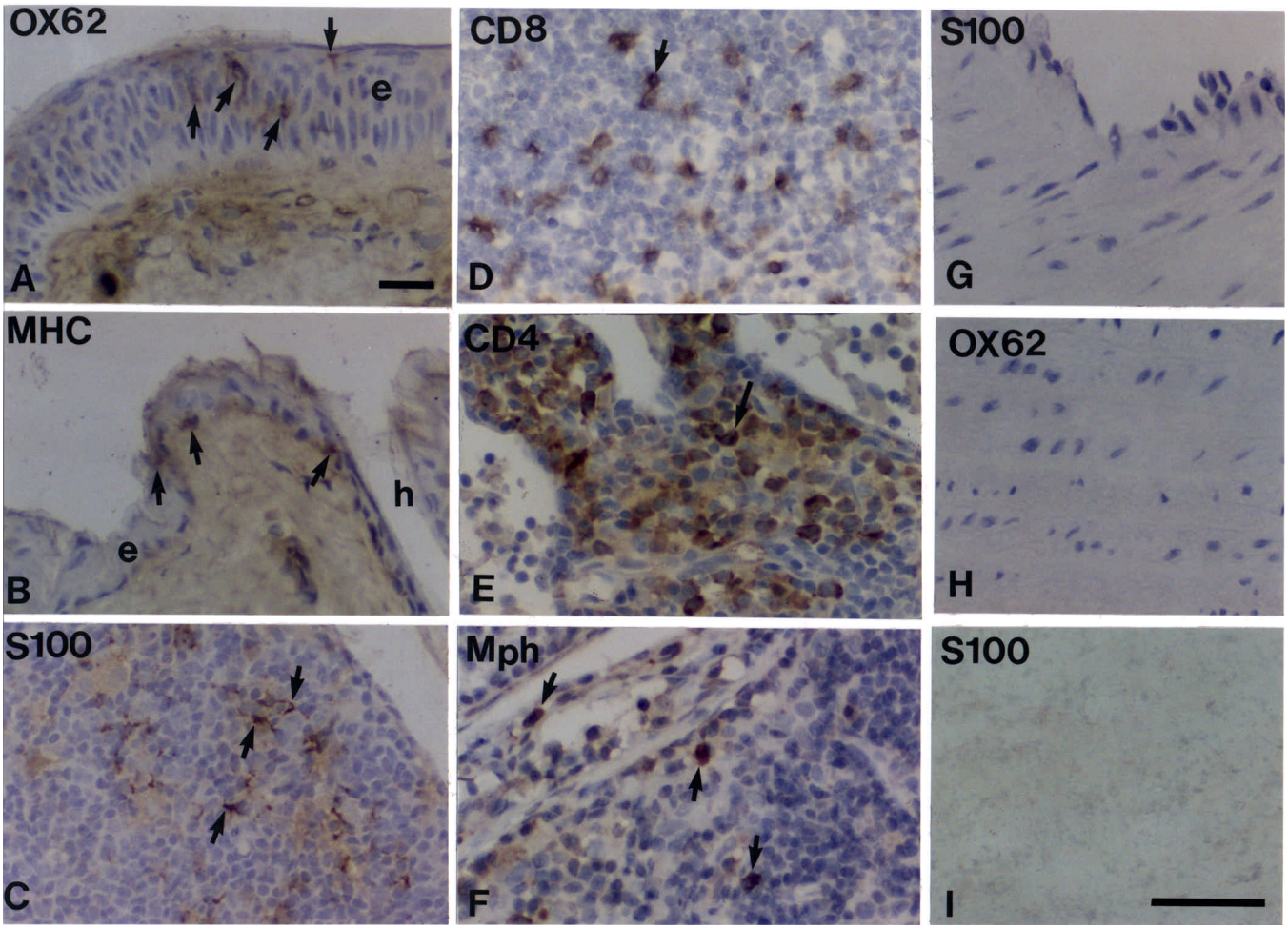

Fig. 1. Positive and negative controls for antibodies used in the study. **A.** Positive control on rat skin for OX-62 immunoreactivity. The immunostained cells (arrows) are epidermal Langerhans cells. e: epidermis. **B.** MHC class II positive controls on rat skin showing Langerhans cells (arrows). e: epidermis; h: hair. **C.** Para-aortic lymph node section showing S100 staining by interdigitating dendritic cells (arrows). **D.** $CD8^+$ T cells (arrow) in lymph node. **E.** $CD4^+$ T-cells in T-cell zone of lymph node. **F.** Rat macrophage HIS 36 antibody-positive macrophages (arrows) in lymph node. **G and H.** Negative controls for S100 **(G)**, OX-62 **(H)** performed on sections. **A-H:** ABC immunoperoxidase method, counterstained with Mayer's hematoxylin, Bars: 5µm. **I:** Negative control for S100 in an *en face* specimen, Bar: 20 µm.

series (50%, 70%, 90%, and 100%), finishing with 100% acetone. The segments were infiltrated with increasing concentrations of acetone to Epoxy-Durcupan resin (Fluka) over 3 days (1:1, 1:3, 1:7, 100%), and polymerized in a 70 °C oven for 2 days.

Semithin sections were cut using a Reichert-Jung Ultracut E ultramicrotome and stained with 1% toluidine blue in 1% sodium tetraborate and were then examined under light microscopy to guide the choice of region for ultrathin sections. The selected regions were areas of aortic intima showing no signs of atherosclerosis and aorta displaying atherosclerotic transformation.

From each Durcupan block, eight to ten ultrathin sections were cut using a Reichert-Jung Ultracut E ultramicrotome. The sections were collected on copper grids and stained with 1% lead citrate for 15-20 min. The excess lead citrate was removed by washing the sections in distilled water for 1 min and then air-drying. These stained sections were then examined with the aid of a Hitachi H7000 transmission electron microscope at an accelerating voltage of 75kV.

Results

Analysis of blood cholesterol and triglycerides

At 20 weeks, mean plasma triglyceride levels showed little change in experimental rats (2.7±1.5 mmol/L (mean ± SD)) compared to control rats (2.1±0.67 mmol/L). However, mean cholesterol levels of the experimental rats sacrificed at 20 weeks on the atherogenic diet exceeded that of the control rats eight fold (11.5±4.4 mmol/L versus 1.4±0.075 mmol/L; $P<0.001$) (Fig. 2A).

At 30 weeks, all experimental rats were hypercholesterolemic with mean serum cholesterol levels exceeding that of control rats by 7 fold (11.5±4.1 mmol/L versus 1.6±0.15 mmol/L; $P<0.001$). However, the mean plasma triglyceride levels showed no significant change in experimental animals (3.8±2.7 mmol/L) compared with control rats (3.3±0.90 mmol/L) (Fig. 2B).

Histopathological changes in the aorta during atherogenesis

Normal aorta

Histological examination showed that the luminal side of the aorta was lined by an endothelial monolayer. The internal elastic lamina was located immediately underneath the endothelium along the entire circumference of the vessel. The tunica media consisted of several concentric layers of smooth muscle cells and extracellular collagenous matrix separated by elastic laminae. The adventitia contained connective tissue and abundant adipose tissue, as well as blood vessels and nerves, which supplied the media and adventitia. No spontaneous atherosclerotic changes were detected in the aortas of the healthy rats.

Atherosclerotic aorta

Histological examination of hematoxylin and eosin stained sections from the experimental rat aortas showed atherosclerotic changes, ranging from diffuse intimal edema to elevated atherosclerotic lesions. These lesions created an intima between the endothelial monolayer and internal elastic lamina. Aortas affected by early atherosclerotic changes (10 weeks) displayed diffuse intimal edema. The intima of such lesions contained few cells of variable shape and a homogeneous eosinophilic matrix. Unlike the other smooth muscle cell layers, the layer directly beneath the internal elastic lamina contained smooth muscle cells orientated perpendicular to the plane of the elastic laminae, suggesting a possible response to early atherosclerotic transformation within the intima. The same pattern was also present in areas of aorta exhibiting early lesions that had the appearance of fatty streaks. There were a greater number of stained nuclei in the fatty streak lesions suggesting more cells

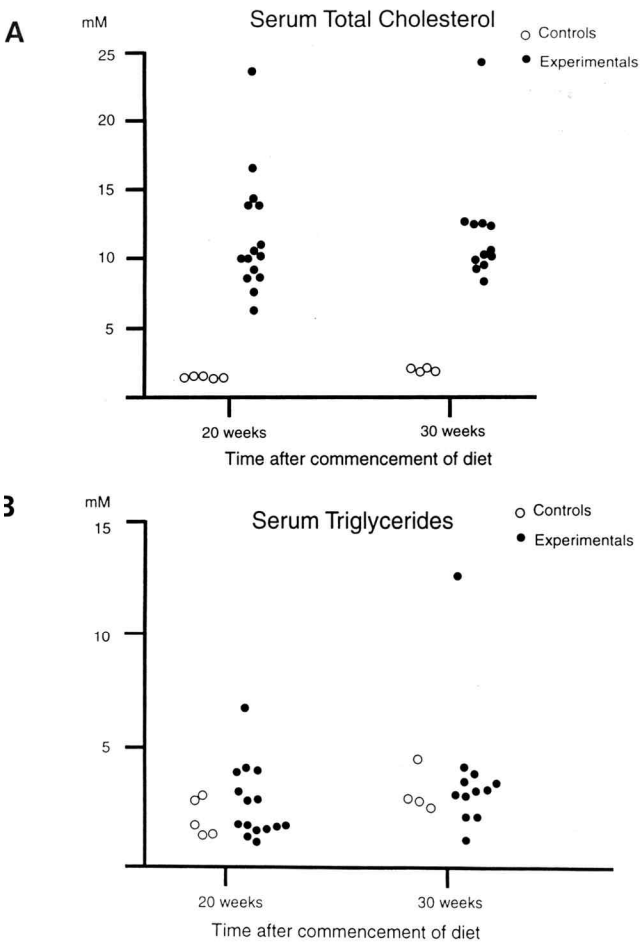

Fig. 2. Serum total cholesterol **(A)** and triglycerides **(B)** levels in rats kept on the atherogenic diet for 20 and 30 weeks.

present than in edematous intimal areas. Within these atherosclerotic lesions, cells of variable shape ranging from elongated to oval or round were noted. The cells were mononuclear with most exhibiting a vacuolated cytoplasm, which gave them the appearance of foam cells. Toluidine blue stained semithin sections revealed some disruption of the internal elastic lamina at sites affected by atherosclerosis.

In the 30-week rat aortas, areas displaying no evidence of atherosclerotic change (athero-resistant) were examined and compared to sites affected by atherosclerosis (athero-prone). In the athero-resistant areas, the aortic wall appeared normal; the endothelial monolayer showed no degenerative changes with no subendothelial lipid accumulation. No histological changes in the smooth muscle layers were detected. In athero-prone areas, however, endothelial denudation was commonly detected, with obvious changes to the intima and media.

Three main types of atherosclerotic lesions were identified. The first (Type I) displayed early destabilization in the intima with a maximum of two cell layers, containing foam cells, situated in the subendothelial space. In the medial layer, there were several foci of smooth muscle cell destruction. This type was observed in thoracic, abdominal, as well as arch of aorta. The second type (Type II) was mainly found in the aortic arch where lesions were more advanced in

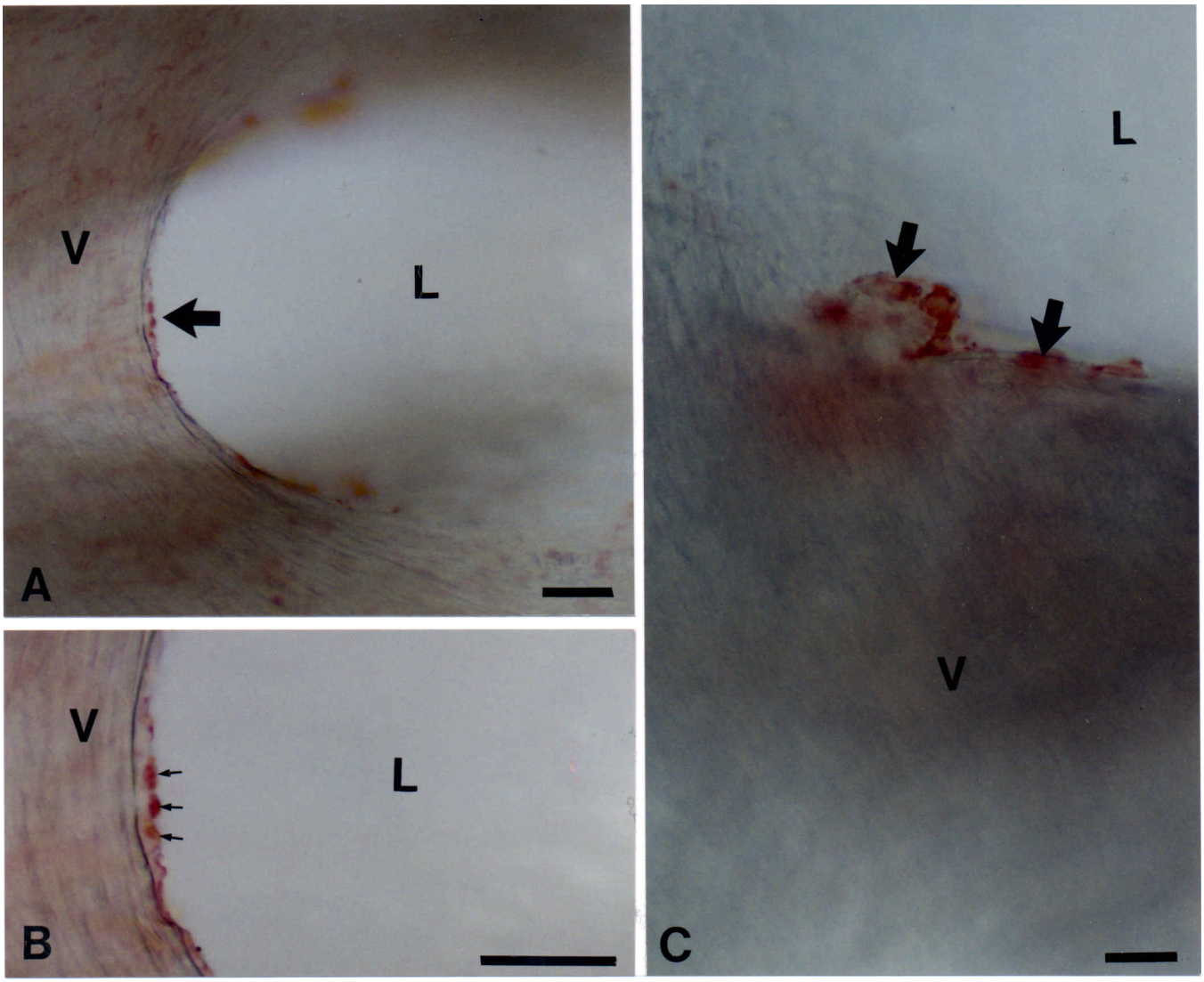

Fig. 3. S100$^+$ cells located around a visceral branch-point visualized in *en face* aortic specimens taken from rats kept on atherogenic diet for 10 weeks. **A.** A group of S100$^+$ cells (arrow) seen along a branch-point of the aorta. Bar: 25 µm. **B** is a detail of **(A)**. Bar: 20 µm. **C.** A cluster of S100$^+$ cells (arrows) located at a visceral aortic branch-point. Bar: 5 µm. V: aortic wall; L: lumen of the aortic visceral branch.

atherosclerotic rats. Most of the lesions occurred at the aortic wall associated with the pulmonary artery and at the orifice of the brachiocephalic artery, where there was considerable intimal expansion. The intima contained mononuclear cells, foam cells, and some smooth muscle cells, with the internal elastic lamina often disrupted. Neutrophilic or eosinophilic inflammation was absent. The media contained foci of smooth muscle cell

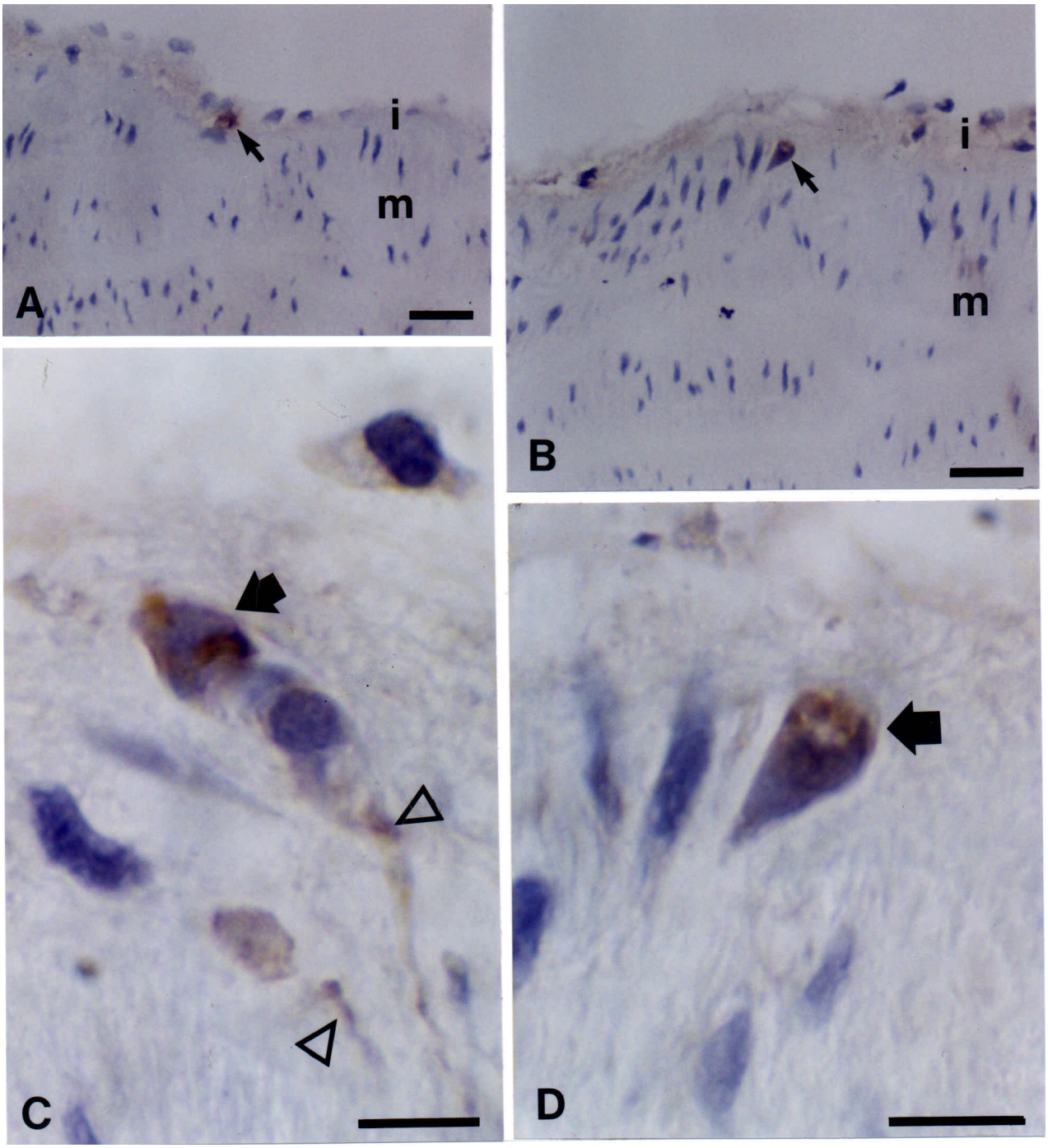

Fig. 4. S100$^+$ cells in Type I and Type II atherosclerotic lesions in hypercholesterolemic rats. **A, B and D** show the appearance and location of S100$^+$ cells (arrows) in Type I atherosclerotic lesions. **(D)** is a detail of **(B)**. i: intima; m: media. **C.** A high magnification image showing the distribution of S100 protein in the cell body (solid arrow) and cellular processes (open arrows) in a Type II atherosclerotic lesion. ABC immunoperoxidase technique, counterstained with Mayer's hematoxylin. Bars: A, B, 5µm; C, D, 2 µm.

destruction but there were no signs of invasion by blood mononuclear cells or the presence of foam cells within the media or the adventitia. The most advanced lesions (Type III) resembled early non-complicated human atherosclerotic plaques, although fibrous caps were not present in the rat aortic lesions. The intima contained a mononuclear infiltrate, smooth muscle cells, and numerous foam cells. Areas of medial smooth muscle cell degeneration were more frequent in type III than the type II. There was no evidence of peri-adventitial or medial inflammation.

Identification of DCs in rat atherosclerotic lesions

En face immunohistochemistry

Examination of *en face* immunostained aortic segments revealed $S100^+$ cells in the aortic intima of all the experimental rats kept on the atherogenic diet for 10 weeks (Fig. 3A-C). In contrast, no $S100^+$ cells were found in the aortic intima of healthy rats. The $S100^+$ cells were distributed irregularly throughout the aorta, but were often seen to form cell clusters. In each of these

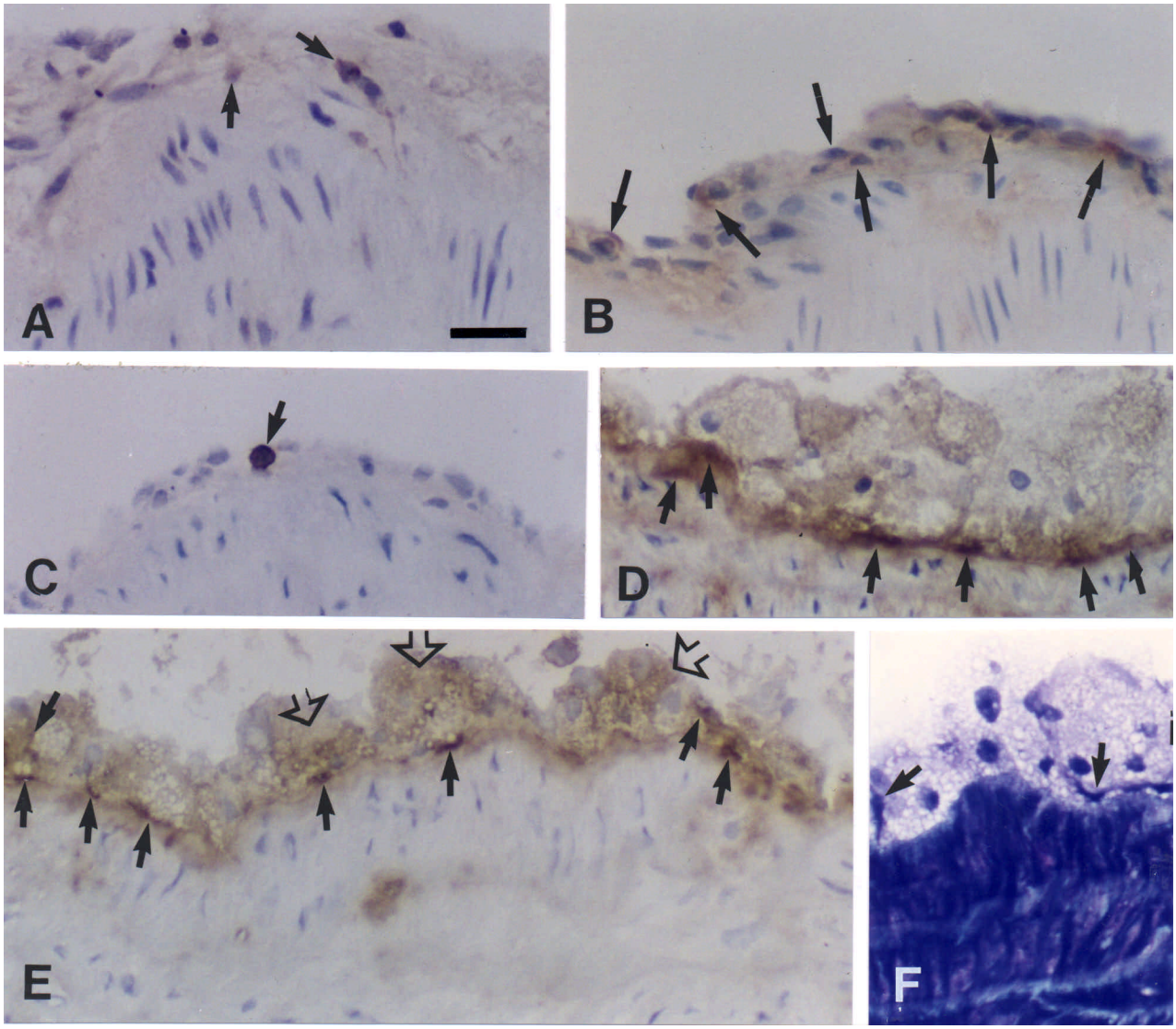

Fig. 5. Distribution of dendritic cells, T cells and macrophages in Type II and Type III atherosclerotic lesions in hypercholesterolemic rats. **A).** $S100^+$ cells in Type II lesions. A detail of this figure is presented in Fig. 4C. **B and C.** Arrows show the accumulation of $CD4^+$ **(B)** and $CD8^+$ cells **(C)** in Type II lesions. The number of $CD4^+$ cells was much greater than that of $CD8^+$ cells. **D.** OX-62^+ cells (arrows) predominantly located on the border between the media and atherosclerotic intima in a Type III lesion. **E.** Intense expression of MHC class II on the border between the media and atherosclerotic intima. Solid arrows show cells that strongly express MHC class II, while open arrows show foam cells, which display moderate degrees of MHC class II expression. **(A-E)** ABC immunoperoxidase technique, counterstaining with Mayer's hematoxylin. **F.** Semithin section showing the typical structure of Type III atherosclerotic lesions; staining with toluidine blue. Intensely stained non-foam cells are shown by arrows. Bars: 5 µm.

clusters, there were usually three to five $S100^+$ cells of variable appearance. These cells had a clearly discernible round to oval shaped cell body and cellular processes. The $S100^+$ cells were often detected at arterial branch-points and tended to be arranged in crescents distal to the origin of the visceral arteries (Fig. 3A-C). There were variable numbers of $S100^+$ cells at these sites, with at least two to three cells present around each arterial branch-point. Some $S100^+$ cells were also distributed longitudinally in clusters along the aorta. At 20 and 30 weeks since the commencement of the atherogenic diet, most of the $S100^+$ cells were found to be co-localized with lipid-laden cells in atherosclerotic lesions located usually at visceral branch-points.

Section immunohistochemistry

Immunohistochemical staining confirmed the presence of $S100^+$ cells within the intimal areas affected by atherosclerotic changes. In both Type I and Type II lesions, $S100^+$ cells were mainly located in the superficial portion of the intima (Fig. 4A,B, 5A). The shape of the $S100^+$ cells ranged from round to elongate with S100 protein distributed in the cell bodies and their cellular processes (Fig. 4C,D). In Type III atherosclerotic lesions, $S100^+$ cells were distributed throughout the intima but were predominantly located at the border of the intima and media and were closely associated with foam cells.

In the present study we also examined the expression of S100α and S100ß sub-units of S100 protein in rat atherosclerotic lesions. The $S100^+$ cells were found to express only S100ß in all types of atherosclerotic lesions.

Analyzing parallel sections we found that $S100^+$ cells were located in areas enriched with both $CD4^+$ T-cells and $CD8^+$ T-cells (Fig. 5A-C). However, we noted that in all types of atherosclerotic lesions the number of $CD4^+$ T-cells was markedly greater than that of $CD8^+$ T-cells, with some lesions containing only a few (Fig. 5C) or even no $CD8^+$ T-cells. In Type I and II atherosclerotic lesions, both $S100^+$ cells and $CD4^+$ cells were mostly located in the subendothelial layer. In contrast, in Type III atherosclerotic lesions both the cell types were located throughout the lesions with predominant localization of $S100^+$ cells on the border between the media and atherosclerotic intima. Analysis of parallel consecutive sections stained with antibodies to S100, OX-62, and MHC Class II revealed that $S100^+$ cells were immunopositive for antibodies to OX-62 and MHC Class II. In Type III atherosclerotic lesions, $OX\text{-}62^+$ cells were predominantly located on the border between the media and atherosclerotic intima (Fig. 5D). Similarly, intense expression of MHC class II was detected in the same location (Fig. 5E). Apart from strong expression of MHC class II by $OX\text{-}62^+$ cells, a moderate degree of MHC class II was also evident in foam cells (Fig. 5E). $OX\text{-}62^+/I^+$ cells corresponded to cells intensely stained with toluidine blue in semithin sections (Fig. 5F).

Semiquantitative data on the cell composition in different types of atherosclerotic lesions is shown in Table 3.

Table 3. Cell composition in different types of atherosclerotic lesions in hypercholesterolemic rats.

TYPE OF LESION	CELLTYPES*		
	Macrophage/foam cells	T-cells	Dendritic cells
Type I	+++	++	+
Type II	+++++	+++	+
Type III	++++++	+++	+

*: semiquantitative graduating scale (+ to ++++++) for estimation of cell numbers in atherosclerotic lesions

Ultrastructural analysis

In the subendothelial layer of the aortas of rats kept on the atherogenic diet for 10 weeks, cells with the characteristics typical of DCs were detected (Fig. 6A-C). Low differentiated cells containing slightly angulated nuclei with chromatin condensed around the nuclear membrane were identified as immature DCs by the presence of a few tubular cisterns located on one pole of the cells (Fig. 6A), a typical feature of immature DCs (Bobryshev and Lord, 1995b, 1996). These cells contained short microvilli, a few mitochondria and ribosomes but lacked secondary lysosomes and phagolysosomes (Fig. 6A).

Moderately differentiated DCs were characterized by the presence of a tubulovesicular system, which was mostly located in the cell body around the nucleus. In different poles of the perinuclear cytoplasm, there were variations in the tubulovesicular system development with the tubulovesicular system typically well formed only at one pole (Fig. 6C). At another cell pole, the tubulovesicular system characteristically contained only one or two elongated tubular cisterns showing a crescent pattern around the nucleus (Fig. 6D). Moderately

Fig. 6. Ultrastructural identification of dendritic cells in the subendothelial layer of the edematous intima in hypercholesterolemic rats. **A.** A low differentiated cell containing slightly angulated nucleus (N) with chromatin condensed around the nuclear membrane. The cell possesses short microvilli and a few cistern tubules (arrows) located on one pole of the cell. **B** shows a moderately differentiated dendritic cell. **C** represents a detail of B. The most characteristic feature of this cell is the well-developed network of tubular cisterns forming together with vesicles a tubulovesicular system. In **C**, arrows show tubular cisterns. In **B,** large arrows show cellular processes and small arrows show microvillous projections. The cell contains an angulated nucleus (N) and several mitochondria (m) but lacks secondary lysosomes and phagosomes. **D.** A parallel consecutive section showing a long continuous cistern (small arrows) of the tubulovesicular system in the same cell. Large arrows show cell processes. L:- aortic lumen. Bars: 1 µm.

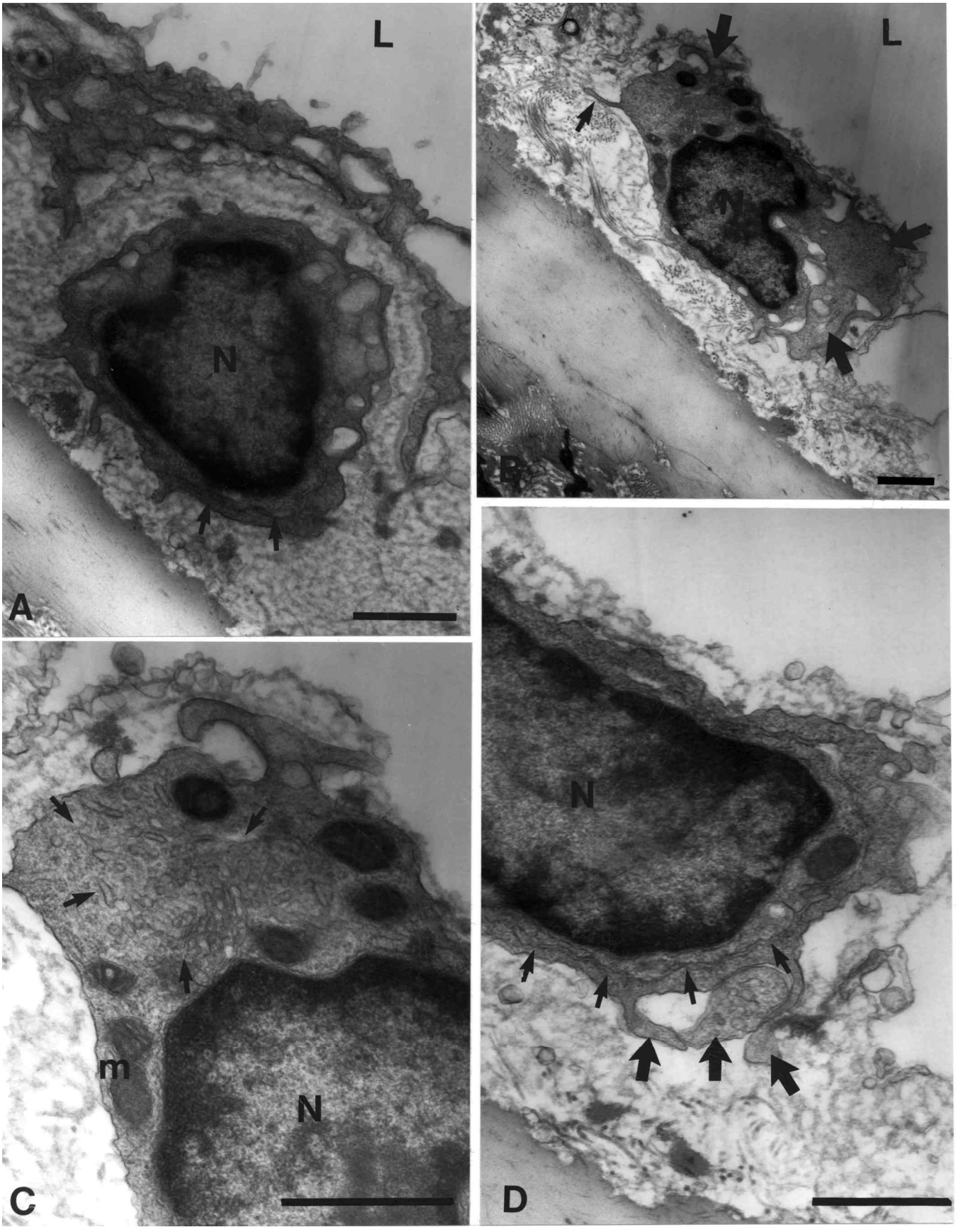
L
N
A
L
B
N
m
N
C
N
D

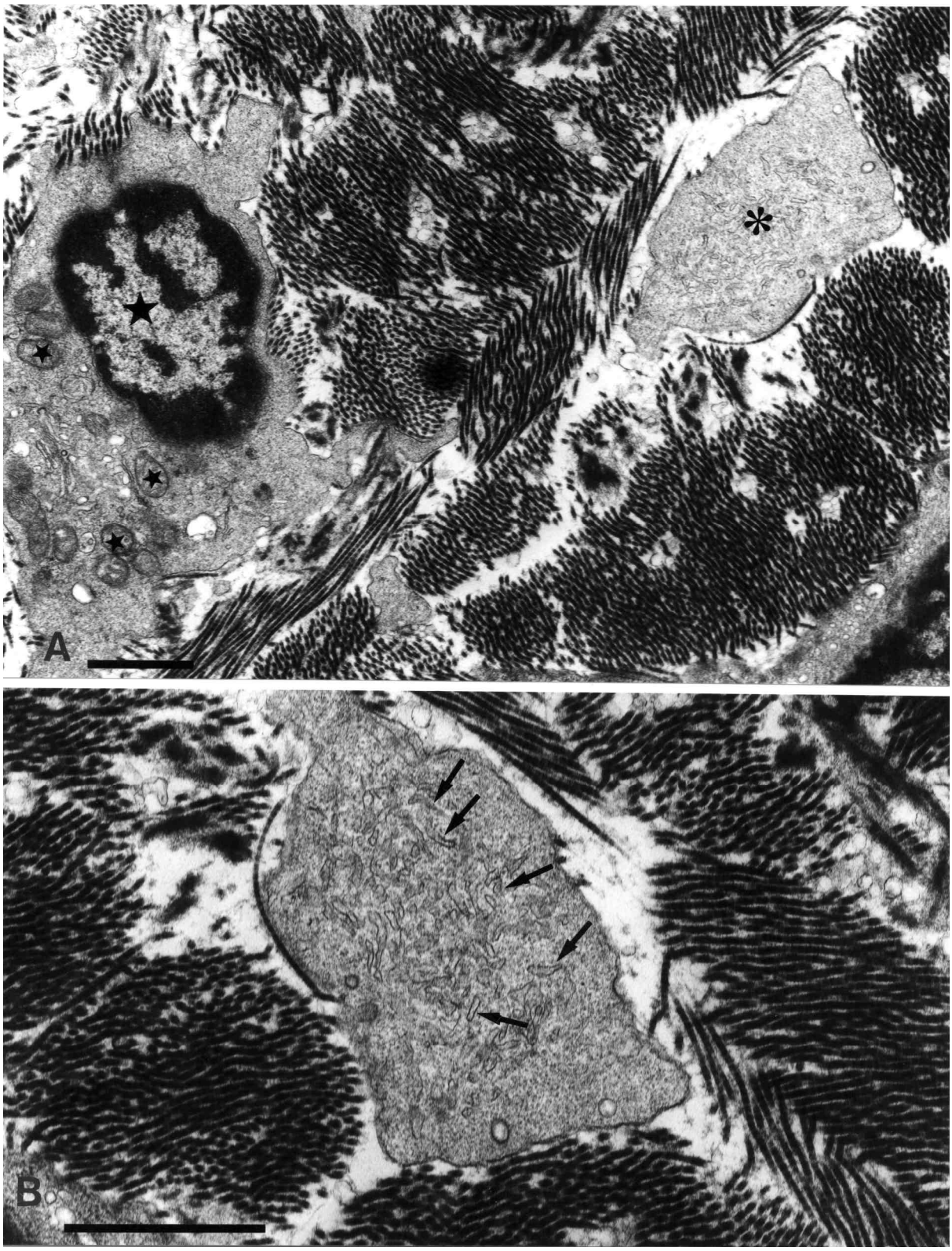

Fig. 7. A well-differentiated dendritic cell and its cell process located in the deep portion of an atherosclerotic lesion between bands of collagen fibers (**A, B**). In **(A)**, the nucleus of the dendritic cell is marked by a large star, while mitochondria are marked by small stars. The cellular process is indicated by an asterisk and its association with the cell body of the dendritic cell was established by analysis of parallel consecutive sections. **B.** Mirror image of the cellular process shown in **(A)** showing hypertrophied cisterns of the tubulovesicular system (arrows). Bars: 1 µm.

differentiated DCs contained microvillous projections and cellular processes (Fig. 6B-D). These cells lacked lysosomes and phagosomes.

Other cells, which were predominantly located in the deep portion of the atherosclerotic intima, displayed features compatible with mature DCs (Fig. 7A). The distinctive feature of these cells was the presence of a well-developed tubulovesicular system mostly developed in cellular processes (Fig. 7A,B). The cellular processes were long and twisted and establishing continuity between the cell body and its cellular processes required the analysis of a set of ultrathin consecutive sections. The cytoplasm of well-differentiated DCs contained a large number of mitochondria but lacked secondary lysosomes and phagolysosomes. Immature and mature DCs possessed no basal lamina around the plasmalemmal membrane (Figs 6A-D, 7A,B).

No cells with a dendritic cell appearance were identified in the aortic intima of healthy rats. Similarly, no cells with a dendritic cell appearance were identified in segments of the aortas of hypercholesterolaemic rats that showed no atherosclerotic alteration.

Discussion

The present study demonstrates for the first time the presence of DCs in atherosclerotic lesions of hypercholesterolemic rats. The evidence of the presence of DCs in rat atherosclerotic lesions was attained from immunohistochemical analysis and from electron microscopic examination. Rat DCs express S100 protein, OX-62 antigen, MHC Class II and posses a well-developed tubulovesicular system, unique to interdigitating DCs (Anderson and Anderson, 1981). In healthy rats, however, no DCs were observed in the intima. In hypercholesterolaemic rats, similarly, no DCs were observed in the athero-resistant areas that did not show signs of atherosclerotic transformation. This might suggest that DCs observed in the atherosclerotic lesions of hypercholesterolaemic rats originate from *blood dendritic cells*. In man, in addition to *blood dendritic cells* that infiltrate the arterial wall during plaque formation, *vascular dendritic cells* (VDCs) that reside in the normal arterial wall are also involved in atherosclerosis (Bobryshev and Lord, 1998; Bobryshev, 2000).

In the present study, DCs were detected in the experimental animals as early as 10 weeks after commencing the diet. The cells were clustered and irregularly distributed through the aorta, but were concentrated at arterial branch-points. In rats kept on the atherogenic diet for 20 and 30 weeks, the distribution of DCs at athero-prone sites was even more striking. The cells were present around the origin of the visceral arteries and in longitudinally orientated clusters along lines connecting the orifices of the aortic branches. This pattern is similar that reported on the distribution of T-cells and macrophages in rats with diet-induced hypercholesterolaemia (Haraoka et al., 1995; Watanabe et al., 1996). In those studies, clusters of T-cells and macrophages were found in areas where lesions develop, namely, in the dorsal wall of the thoracic aorta and around the branch-points of both the thoracic and abdominal aorta (Haraoka et al., 1995; Watanabe et al., 1996). In the present examination, DCs were identified at athero-prone sites, where the accumulation of both T-cells and macrophages occurred.

DCs represent a diverse population of specialized antigen presenting cells with a powerful capacity for initiating the primary T-cell response (King and Katz, 1990; Steinman, 1991; Kamperdijk et al., 1993; Sprecher and Becker, 1993; Banchereau and Steinman, 1998). Through their direct contacts with T-cells and macrophages, DCs are involved in immune-inflammatory reactions (King and Katz, 1990; Steinman, 1991; Kamperdijk et al., 1993; Sprecher and Becker, 1993; Banchereau and Steinman, 1998). In man, clustering DCs as well as clustering DCs with T-cells have been found in atherosclerosis-prone areas (Bhagwat and Robertson, 1973; Sveden and Eide, 1980) of apparently normal adult arteries (Bobryshev and Lord, 1995b). The concept of vascular-associated lymphoid tissue (VALT), analogous to mucosa-associated lymphoid tissue (MALT) has recently been proposed by Wick and co-workers (1997) with a suggestion that DCs are an essential component of VALT (Wick et al., 1997). VALT has been suggested to screen the vascular tissue for the presence of potentially harmful antigens (Wick et al., 1997). In non-diseased arteries in man, VALT is thought to consist of small numbers of T-cells, macrophages and DCs disseminated throughout the intima (Wick et al., 1997). In the early stages of atherogenesis, VALT becomes hypertrophied in response to pro-atherogenic stimuli (Wick et al., 1997). In rats, VALT seems to form as a novo tissue structure within the intimal layer in rats kept on the atherogenic diet and thus, in contrast to man, the VALT formation in hypercholesterolaemic rats represents a pathophysiological event.

Evidence of the involvement of immunological and inflammatory mechanisms in atherogenesis has been accumulating over the past two decades (Hansson et al., 1989; Libby and Hansson, 1991; Yokota and Hansson, 1995). Macrophages and T-lymphocytes are the two main immunocompetent cells present in atherosclerotic lesions (Hansson et al., 1989; Libby and Hansson, 1991; Ross, 1993; Yokota and Hansson, 1995), where they are intermingled with small numbers of DCs (Bobryshev and Lord, 1996, 1998). In atherosclerosis, DCs have been suggested to be involved in the activation of T-cells (Bobryshev and Lord, 1998; Bobryshev, 2000). The ability of DCs to physically cluster with lymphocytes and macrophages directly within the arterial wall (Bobryshev and Lord, 1998; Bobryshev, 2000) suggests that intravascular clustering might be necessary for the transduction of immune information.

A few observations suggest that DCs accumulate in

aortic lesions in experimental animal models of atherosclerosis (Bobryshev and Lord, 1999; Bobryshev et al., 1999a,b, 2001). DCs have been identified in aortic atherosclerotic lesions in apo-E deficient mice (Bobryshev and Lord, 1999; Bobryshev et al., 1999a, 2001). Although mouse atherosclerosis models are very useful for investigating both the contribution of macrophages in atherogenesis and the mechanisms of foam cell formation, mouse atherosclerosis seems not to completely mimic the immune-inflammatory aspects of human atherosclerosis, as mouse atherosclerotic lesions lack an accumulation of T-lymphocytes (Dansky et al., 1997). In contrast to mouse atherosclerosis, the accumulation of large numbers of both macrophages and T-cells in the aortic intima is a feature of experimental atherosclerosis in hypercholesterolemic rats (Haraoka et al., 1995; Watanabe et al., 1996), which may make this model useful for investigating the contribution of DCs in atherogenesis.

Acknowledgements. We thank the St. Vincent's Clinic Foundation, Sydney, for financial support.

References

Anderson A.O. and Anderson N.D. (1981). Structure and physiology of lymphatic tissues. In: Cellular functions in immunity and inflammation. Oppenheim J.J., Roenstreich D.L and Potter M. (eds). Edward Arnold. London. pp 29-76.

Banchereau J. and Steinman R.M. (1998). Dendritic cells and the control of immunity. Nature 392, 245-252.

Belliveau R. and Marsh M.E. (1961). Effects of sodium chloride in rats fed an atherogenic diet. Arch. Pathol. 71, 559-565.

Bhagwat A.G. and Robertson A.L. (1973). Distribution and severity of atherosclerotic lesions in the human thoracic aorta. Angiology 24, 81-190.

Bobryshev Y.V. (2000). Dendritic cells and their involvement in atherosclerosis. Curr. Opin. Lipidol. 11, 511-517.

Bobryshev Y.V. and Lord R.S.A. (1995a). S-100 positive cells in human arterial intima and in atherosclerotic lesions. Cardiovasc. Res. 29, 689-696.

Bobryshev Y.V. and Lord R.S.A. (1995b). Ultrastructural recognition of cells with dendritic cell morphology in human aortic intima. Contacting interactions of vascular dendritic cells in athero-resistant and athero-prone areas of the normal aorta. Arch. Histol. Cytol. 58, 307-322.

Bobryshev Y.V. and Lord R.S.A. (1996). Structural heterogeneity and contacting interactions of vascular dendritic cells in early atherosclerotic lesions of the human aorta. J. Submicrosc. Cytol. Pathol. 28, 49-60.

Bobryshev Y.V. and Lord R.S.A. (1998). Mapping of vascular dendritic cells in atherosclerotic arteries suggests their involvement in local immune-inflammatory reactions. Cardiovasc. Res. 37, 799-810.

Bobryshev Y.V. and Lord R.S.A. (1999). Atherosclerotic lesions of apolipoprotein E deficient mice contain cells expressing S100 protein. Atherosclerosis 143, 451-454.

Bobryshev Y.V., Lord R.S.A., Rainer S., Jamal O.S. and Munro V.F. (1996a). Vascular dendritic cells and atherosclerosis. Pathol. Res. Pract. 192, 462-467.

Bobryshev Y.V., Lord R.S.A., Rainer S.P. and Munro V.F. (1996b). VCAM-1 expression and network of VCAM-1 positive vascular dendritic cells in advanced atherosclerotic lesions of carotid arteries and aortas. Acta. Histochem. 98, 185-194.

Bobryshev Y.V., Lord R.S.A. and Watanabe T. (1997). Structural peculiarities of vascular dendritic cell tubulovesicular system in human atherosclerotic aorta. J. Submicrosc. Cytol. Pathol. 29, 553-561.

Bobryshev Y.V., Babaev V.R., Lord R.S.A. and Watanabe T. (1999a). Ultrastructural identification of cells with dendritic cell appearance in atherosclerotic aorta of apolipoprotein E deficient mice. J. Submicrosc. Cytol. Pathol. 31, 527-531.

Bobryshev Y.V., Konovalov H.V. and Lord R.S.A. (1999b). Ultrastructural recognition of dendritic cells in the intimal lesions of aortas of chickens affected with Marek's disease. J. Submicrosc. Cytol. Pathol. 31, 179-185.

Bobryshev Y.V., Taksir T., Lord R.S.A. and Freeman M.W. (2001). Evidence that dendritic cells infiltrate atherosclerotic lesions in apolipoprotein E deficient mice. Histol. Histopathol. 16, 801-808.

Buelens C., Verhasselt V., De Groote D., Thielemans K., Goldman M. and Willems F. (1997). Human dendritic cell responses to lipopolysaccharides and CD40 ligation are differentially regulated by IL-10. Eur. J. Immunol. 27, 1848-1852.

Dansky H.M., Charlton S.A., Harper M.G. and Smith J.D. (1997). T and B lymphocytes play a minor role in atherosclerotic plaque formation in the apolipoprotein E-deficient mouse. Proc. Natl. Acad. Sci. USA 94, 4642-4646.

Hansson G.K., Holm J. and Jonasson L. (1989). Detection of activated T-lymphocytes in the human atherosclerotic plaque. Am. J. Pathol. 135, 169-175.

Haraoka S., Shimokama T. and Watanabe T. (1995). Participation of T-lymphocytes in atherogenesis: sequential and quantitative observations of aortic lesions of rats with diet-induced hypercholesterolaemia using *en face* double immunostaining. Virchows Arch. 426, 307-315.

Hart D.N. (1997). Dendritic cells: unique leucocyte populations which control the primary immune response. Blood 90, 3245-3287.

Hart D.N. and Fabre J.W. (1981). Major histocompatibility complex antigens in rat kidney, ureter, and bladder. Localisation with monoclonal antibodies and demonstration of Ia-positive dendritic cells. Transplantation 31, 318-325.

Hsu S-M., Raine L. and Fanger H. (1981). Use of avidin-biotin-peroxidase complex (ABC) in immunoperoxidase techniques: a comparison between ABC and unlabeled antibody (PAP) procedures. J. Histochem. Cytochem. 29, 577-580.

Inaba K., Metlay J.P., Crowley M.T. and Steinman R.M. (1990). Dendritic cells pulsed with protein antigens *in vitro* can prime antigen-specific, MHC-restricted T-cells in situ. J. Exp. Med. 172, 631-640.

Kamperdijk E.W., Arkema J.M., Verdaasdonk M.A., Beelen R.H. and van Vugt E. (1993). Rat thymic dendritic cells. In: Dendritic cells in fundamental and clinical immunology. Kamperdijk E.W., Nieuwenhuis P. and Hoefsmit E.C. (eds). Advances in Experimental Medicine and Biology. Vol. 329. Plenum Press. New York-London. pp 141-146.

King P.D. and Katz D.R. (1990). Mechanisms of dendritic cell function. Immunol. Today 11, 206-211.

Knight S.C., Krejci J., Malkovsky M., Colizzi V., Gautum A. and

Asherson G.L. (1985). The role of dendritic cells in the initiation of immune responses to contact sensitizers. In vivo exposure to antigen. Cell Immunol. 94, 427-434.

Libby P. and Hansson G.K. (1991). Involvement of the immune system in human atherogenesis: Current knowledge and unanswered questions. Lab. Invest. 64, 5-15.

Macatonia S.E., Knight S.C., Edwards A.J., Griffiths S. and Fryer P. (1987). Localization of antigen on lymph node dendritic cells after exposure to the contact sensitizer fluorescein isothiocyanate. Functional and morphological studies. J. Exp. Med. 166, 1654-1667.

Ozmen J., Lord R.S.A., Bobryshev Y.V., Ashwell K.W.S. and Munro V.F. (1998). S100 protein is expressed in induced atherosclerotic lesions of hypercholesterolaemic rats. Biomed. Res. 19, 279-281.

Pure E., Inaba K., Crowley M.T., Tardelli L., Witmer-Pack M.D., Ruberti G., Fathman G. and Steinman R.M. (1990). Antigen processing by epidermal Langerhans cells correlates with the level of biosynthesis of MHC class II molecules and expression of invariant chain. J. Exp. Med. 172, 1459-1469.

Romani N. and Schuler G. (1992). The immunologic properties of epidermal Langerhans cells as part of the dendritic cell system. Springer Semin. Immunopathol. 13, 256-279.

Ross R. (1993). The pathogenesis of atherosclerosis: a perspective for the 1990s. Nature 362, 801-809.

Sallusto F. and Lanzavecchia A. (1995). Dendritic cells use macropinocytosis and the mannose receptor to concentrate antigen to the MHC class II compartment. Down regulation by cytokines and bacterial products. J. Exp. Med. 182, 389-400.

Sprecher E. and Becker Y. (1993). Role of Langerhans cells and other dendritic cells in disease states. In vivo 7, 217-227.

Steinman R.M. (1991). The dendritic cell system and its role in immunogenicity. Annu. Rev. Immunol. 9, 271-296.

Steinman R.M. and Cohn Z.A. (1973). Identification of a novel cell type in peripheral lymphoid organs of mice. I. Morphology, quantitation, tissue distribution. J. Exp. Med. 137, 1142.

Steinman R.M., Lustig D.S. and Cohn Z.A. (1974). Identification of a novel cell type in peripheral lymphoid organs of mice. III. Functional properties in vivo. J. Exp. Med. 139, 1431.

Sveden T. and Eide T.J. (1980). Distribution of atherosclerosis in human descending thoracic aorta. A morphometric study. Acta Pathol. Microbiol. Scand. 88, 97-103.

Watanabe T., Haraoka S. and Shimokama T. (1996). Inflammatory and immunological nature of atherosclerosis. Int. J. Cardiol. 54, S51-S60.

Wick G., Romen M., Amberger A., Metzler B., Mayr M., Falkensammer G. and Xu Q. (1997). Atherosclerosis, autoimmunity, and vascular-associated lymphoid tissue. FASEB J. 11, 1199-1207.

Winzler C., Rovere P., Rescigno M., Granucci F., Adorini L., Zimmermann V.S., Davoust J. and Ricciardi-Castagnoli P. (1997). Maturation stages of mouse dendritic cells in growth factor-dependent long-term cultures. J. Exp. Med. 185, 317-328.

Yokota T. and Hansson G.K. (1995). Immunological mechanisms in atherosclerosis. J. Intern. Med. 238, 479-489.

Accepted November 6, 2001